Korean Chem. Eng. Res., 55(1), 130-134 (2017)
https://doi.org/10.9713/kcer.2017.55.1.130
PISSN 0304-128X, EISSN 2233-9558

Morphology of Sub-Microscale Atmospheric Aerosols composed of Two Liquid Phases According to the Loading Ratio of Organics/Water

Kee-Youn Yoo†

Department of Chemical and Biomolecular Engineering, Seoul National University of Science and Technology, 232, Gongneung-ro, Nowon-gu, Seoul, 01811, Korea
(Received 12 October 2016; Received in revised form 23 November 2016; accepted 5 December 2016)

Abstract – Organic aerosols dispersed in the atmosphere likely undergo phase separation. Such internally mixed particles are often described as comprising an organic phase and an aqueous phase separately. We studied the morphology of two liquid separated aerosols in the sub-microscale by using a simple thermodynamic model with Russian doll geometry. The morphology of particles can be easily predicted from the simple criteria on the surface tension and two algebraic equations (the volume constraint and Young equation). This result may give the potential explanation about the complex morphology of the organic airborne particles

Key words: Atmospheric organic aerosol, Morphology, Liquid-liquid separation, Russian doll model

1. Introduction

Aqueous aerosol particles, including organic species, are prevalent in the ambient atmosphere [1,2]. Such atmospheric particles may undergo liquid-liquid phase separation due to the immiscibility [3-6]. This phase separation transforms the morphology of particles, and then they are no longer homogeneous single spheres. The tangible morphology is determined fundamentally by the balance of molecular interactions among the various chemical constituents in the droplet. Experimental and optical studies report the formation of core-shell structure with surface-active organics and asymmetric, overlapped spheres [6,7]. The morphology of sub-microscale particles containing two immiscible liquids is of significant interest, although perplexing to verify experimentally, due to the impact on the physical/optical properties, the rate of gas and water uptake and the kinetics of heterogeneous reactions in ambient atmosphere [8]. By now, most computational researches focus on the calculation of phase equilibria of inorganic/organics [9-12]. However, knowledge of the morphology of phase separated organic aerosols is still largely uncertain. Aerosol particles affect the earth's energy budget directly by scattering and absorbing solar radiation and indirectly by acting as cloud condensation nuclei [13]. Then the physical state and morphology of particles might be critical to estimate the aerosol effects on climate.

We used a simplified thermodynamic model that minimizes the Gibbs free energy of a liquid-liquid segregated particle with a Russian doll droplet representation [14,15] and conducted computational studies to examine the effect of relative loading ratio of water and organic species with respect to the morphology of sub-microscale liquid-liquid separated atmospheric aerosols. Thus, we can explain the reported experimental morphologies with the surface tension between two liquids and the air and the relative loading ratio of organics/water [4,6,16-18] and suggest that such morphologies might also exist in tropospheric aerosols. And we can construct a predictive atmospheric aerosol module to estimate the effects on the radiative forcing, considering the possible configuration of organic aerosol with phase separation.

2. Russian Doll Representation of two Liquid Phase Separated Aerosol

We first assume that aqueous phase forms a sphere that is partially wetted by organic-rich phase in sub-micro-scale. Called the Russian doll (RD) or lens-on-sphere model [14,15], it is shown in Fig. 1. For all droplets, we also assume that, under the fixed volume of each liquid, the Laplace terms are constants irrespective of the degree of insertion between two liquid phases and then can be neglected in the thermodynamic model. Hence the Gibbs free energy of two liquid phase separated aerosol can be formulated from the idealized geometry of the RD model:

$$\Delta G = \gamma_{wv}A_{wv} + \gamma_{ov}A_{ov} + \gamma_{wo}A_{wo} . \quad (1)$$

We use the subscripts *w*, *o* and *v* to refer to the aqueous and organic-rich phases and vapor, respectively, and the two liquid phases can be any pair of liquid region identified to have a homogeneous interior. The actual *wo* interface could have an intermediate curvature between the idealized RD and a flat surface, determined by the equilibrium between elastic and capillary forces in aerosol. But the intermediate curvature gives almost the same configura-

† To whom correspondence should be addressed.
E-mail: kyyoo@seoultech.ac.kr

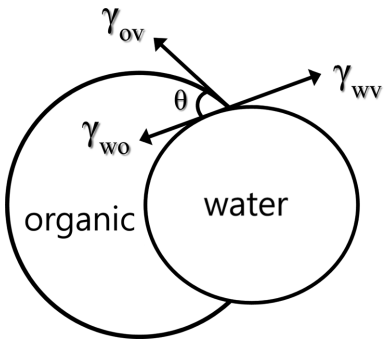

Fig. 1. Russian doll model of two liquid phase segregated aerosol with partial wetting.

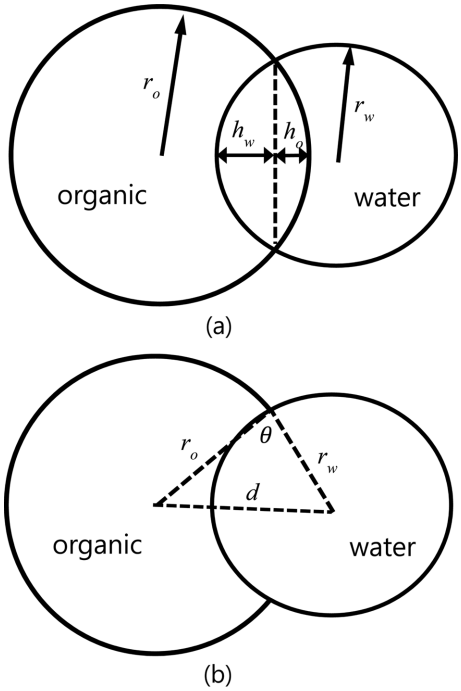

Fig. 2. (a) Idealized geometry for a Russian doll model (RD) of two liquid phase segregated aerosol ($0 < h_w < 2r_w$). (b) The contact angle at the RD geometry, in which d ($=r_w - h_w + r_o - h_o$) is the distance between the spherical centers of each phase.

tion as RD model in the sub-microscale. In what follows, we consider the minimization problem of the free energy of the idealized RD model, Eq. (1). Using the radius r_w and r_o of the spherical section of water and organic phases, and the height h_w and h_o of the overlapped spherical caps (See Fig. 2(a)), the free energy of the RD model is:

$$\Delta G = \gamma_{wv}(4\pi r_w^2 - 2\pi r_w h_w) + \gamma_{ov}(4\pi r_o^2 - 2\pi r_o h_o) + 2\gamma_{wo}\pi r_w h_w . \quad (2)$$

Here r_w is constant but r_o is varying according to the degree of insertion of two phases with the fixed volumes, v_w and v_o, of each phase in aerosol. The organic volume balance assuming the constant density is as follows:

$$\frac{4}{3}\pi r_o^3 - \frac{\pi}{6}h_w(3a^2 + h_w^2) - \frac{\pi}{6}h_o(3a^2 + h_o^2) = v_o \quad (3)$$

where

$$a = \sqrt{2r_w h_w - h_w^2},$$

$$h_o = r_o - \sqrt{r_o^2 - a^2} \text{ for } r_o \geq h_o,\ h_o = r_o + \sqrt{r_o^2 - a^2} \text{ for } r_o < h_o .$$

Within this volume constraint, the free energy of the RD model, Eq. (2), is the single function of the height of the aqueous spherical cap, h_w, which characterizes the degree of insertion between two segregated phases. Figs. 3 and 4 show the variation of the free energy according to h_w in two representative systems with equal mass loading, respectively, in the typical atmospheric condition. Fig. 5 gives the cross-sectional equilibrium configuration of nonane/water (partial wetting) and octanol/water (total wetting) corresponding to Figs. 3 and 4, in which the contact angle θ between two

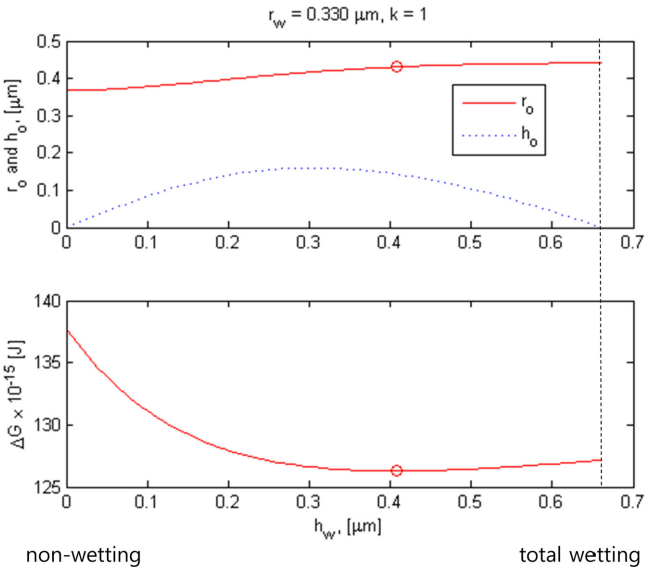

Fig. 3. The variation of r_o and ΔG according to the height of the aqueous spherical cap, h_w, in which circle denotes the equilibrium point (nonane/water system: $v_o = 0.2089\ \mu m^3$, $v_w = 0.1504\ \mu m^3$).

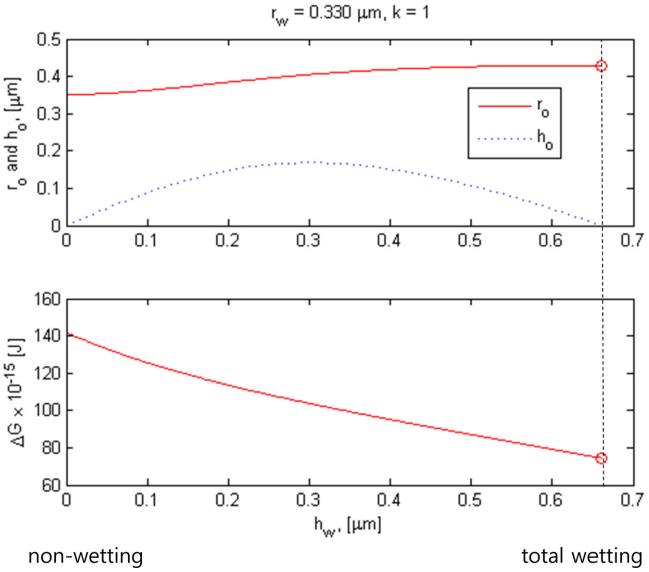

Fig. 4. The variation of r_o and ΔG according to the height of the aqueous spherical cap, h_w, in which circle denotes the equilibrium point (octanol/water system: $v_o = 0.1820\ \mu m^3$, $v_w = 0.1504\ \mu m^3$).

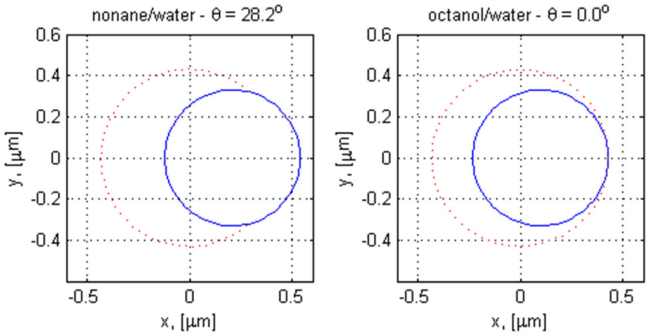

Fig. 5. The cross-sectional equilibrium configurations of two representative liquid-liquid segregated aerosols corresponding to Fig. 3 and 4 (solid line: aqueous phase, dotted line: organic phase): See Table 1 for the physical properties (densities and surface tensions).

Table 1. Surface tensions and densities of nonane/water and octanol/water system

	γ_{wv} [mJ/m^2]	γ_{wo} [mJ/m^2]	γ_{ov} [mJ/m^2]	ρ_o [mJ/m^2]	θ [deg]
Nonane/water	72.4[a]	52.4[b]	22.7[b]	0.728	28.2
Octanol/water[c]	72.8	8.5	27.1	0.824	0

[a][19](T = 295 K), [b][18](T = 295 K), [c][20]

liquid phases is equivalent to the angle between the contact line and the spherical centers of each phase at equilibrium configuration (see Fig. 2(b)):

$$\theta = \cos^{-1}\frac{r_w^2 + r_o^2 - d^2}{2r_w r_o}. \quad (4)$$

3. Criteria of Non-, Partial and Total Wetting

To analyze the impact of surface tensions on the morphology, we rearrange Eq. (2):

$$\Delta G' = 2\pi r_w(\gamma_{wo} - \gamma_{wv})h_w + 2\pi\gamma_{ov}(2r_o^2 - r_o h_o). \quad (5)$$

Here we omit the constant term $4\pi\gamma_{wv}r_w^2$. The derivative of Eq. (5) with respect to h_w is

$$\frac{d\Delta G'}{dh_w} = 2\pi r_w(\gamma_{wo} - \gamma_{wv}) - 2\pi r_o\frac{dh_o}{dh_w}\gamma_{ov} + 2\pi(4r_o - h_o)\frac{dr_o}{dh_w}\gamma_{ov}, \quad (6)$$

in which

$$\frac{dh_o}{dh_w} = -\frac{h_o}{r_o - h_o}\frac{dr_o}{dh_w} + \frac{r_w - h_w}{r_o - h_o}.$$

When the loading ratio of aqueous/organic phases, $k = v_o/v_w$, is fixed, the involved geometric variables are determined at both limiting cases as follows:

Non-wetting condition:

$$h_o \to 0, r_o \to k^{1/3}r_w, \frac{dr_o}{dh_w} \to 0, \frac{dh_o}{dh_w} \to k^{-1/3} \text{ at } h_w \to 0$$

Total wetting condition:

$$h_o \to 0, r_o \to (1+k)^{1/3}r_w, \frac{dr_o}{dh_w} \to 0, \frac{dh_o}{dh_w} \to -(1+k)^{-1/3} \text{ at } h_w \to 2r_w$$

Thus Eq. (6) is evaluated at these boundaries as follows:

Non-wetting condition:

$$\frac{d\Delta G'}{dh_w} = 2\pi r_w(\gamma_{wo} - \gamma_{wv} - \gamma_{ov}) \quad (7)$$

Total-wetting condition:

$$\frac{d\Delta G'}{dh_w} = 2\pi r_w(\gamma_{wo} - \gamma_{wv} + \gamma_{ov}) \quad (8)$$

We can see that, when $\gamma_{wo} > \gamma_{wv} + \gamma_{ov}$, the total free energy increases with the progress of the insertion of two liquid phases ($d\Delta G'/dh_w > 0$) and the two phases will be separated (non-wetting case). When $\gamma_{wv} - \gamma_{ov} < \gamma_{wo} < \gamma_{wv} + \gamma_{ov}$, the insertion between two liquid phases will be advanced and the progress of the wetting will cease between two boundaries (partial wetting case). When $\gamma_{wo} < \gamma_{wv} - \gamma_{ov}$, then $d\Delta G'/dh_w < 0$ at $h_w = 2r_w$ and the total wetting will occur (aqueous phase will be fully covered by organic phase). Then the RD model is substituted into the simple core-shell model.

4. Effect on Morphology to the Loading Ratio Of Water and Organics

We first conducted computational studies to examine the effect of the loading ratio of organics and water, *k*, in case of partial wetting (nonane/water system). Fig. 6 shows that, regardless of *k*, the equilibrium contact angle is identical to Young equation's prediction $\theta = \cos^{-1}((\gamma_{wv} - \gamma_{wo})/\gamma_{ov}) = 28.2°$, in which we may regard the aqueous phase to the non-deformable solid phase. This result indicates that the force balance at the equilibrium contact line is established as follows:

$$\frac{\gamma_{wv} - \gamma_{wo}}{\gamma_{ov}} = \frac{r_w^2 + r_o^2 - d^2}{2r_w r_o} \quad (9)$$

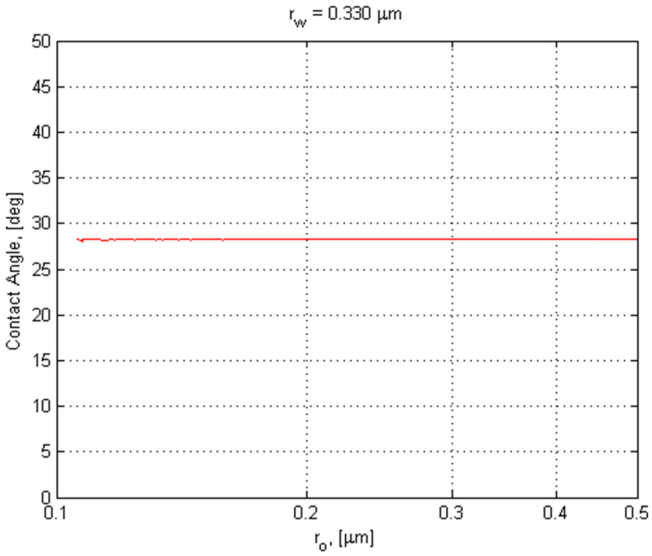

Fig. 6. The contact angle vs. the equilibrium radius of the Russian Doll model according to the loading ratio of nonane/water (The computed contact angle is identical to the Young equation's prediction).

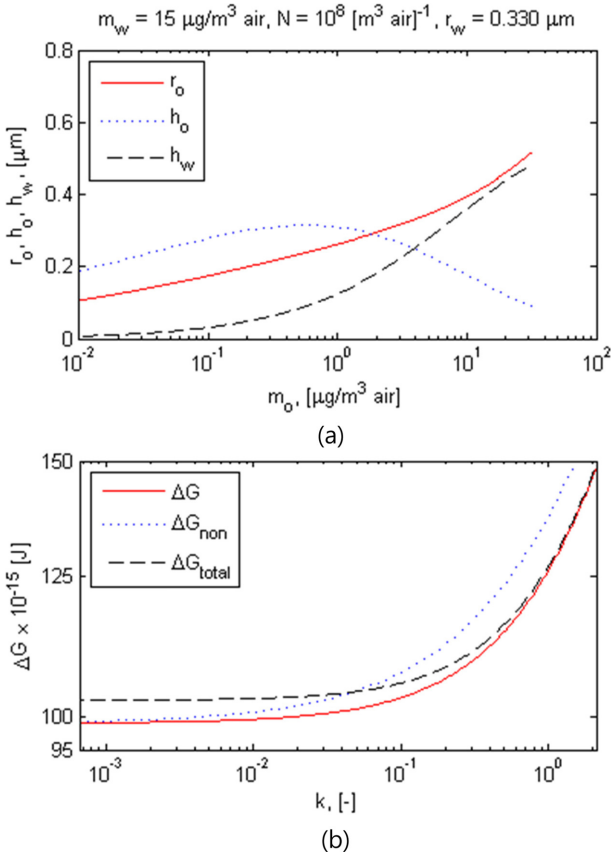

Fig. 7. (a) The variation of the geometric variables of the RD model with respect to the loading weight of organics in nonane/water system. (b) The equilibrium Gibbs free energy of RD model (ΔG), the non-wetting Gibbs free energy (ΔG_{non}), and the total-wetting Gibbs free energy (ΔG_{total}) according to the loading ratio of organics/water in nonane/water system.

Thus, we can also calculate the equilibrium configuration by simultaneously solving Eqs. (3) and (9) with respect to r_o and h_w.

We present the variation of the geometric variables according to the addition of organics in case of partial wetting in Fig. 7(a). In the lower loading, h_o is greater than r_o and increases in step with the additional loading of organics. The cross-sectional equilibrium configurations in Fig. 8 (k = 0.010, 0.038) are partially engulfed in the form of central aqueous phase with lens of organics protruding from one side. And the free energy is comparable with non-wetting case (see Fig. 7(b)). This situation corresponds to the initial introduction of organics to aqueous particles in case of partial wetting. In the high loading, h_o is less than r_o and decreases with the more loading of organics. The free energy approaches to the total wetting case (core-shell configuration). Fig. 8 (k = 2.108) shows that the equilibrium configuration is mostly engulfed (similar to core-shell except that core aqueous phase is positioned at the edge region of organics). In case of total wetting (octanol/water system), the equilibrium configuration is a simple core-shell structure. In the lower loading, the aqueous particles are thinly coated by the organics and the shell side is thicker with the addition of organics (see Fig. 9).

In summary, when liquid-liquid separation in the internally mixed particle occurs, the relative low loading ratio of organics/water results in the organic-film-coated or fatty-ball-protruded aerosol depending on the surface tensions among the aqueous/organic/vapor phases. The high loading ratio gives the core-shell structure with centered or edge-positioned aerosol, apparently, depending on the relations between the surface tensions. These discussions have a correspondence to recent experimental studies [4,6,16-18].

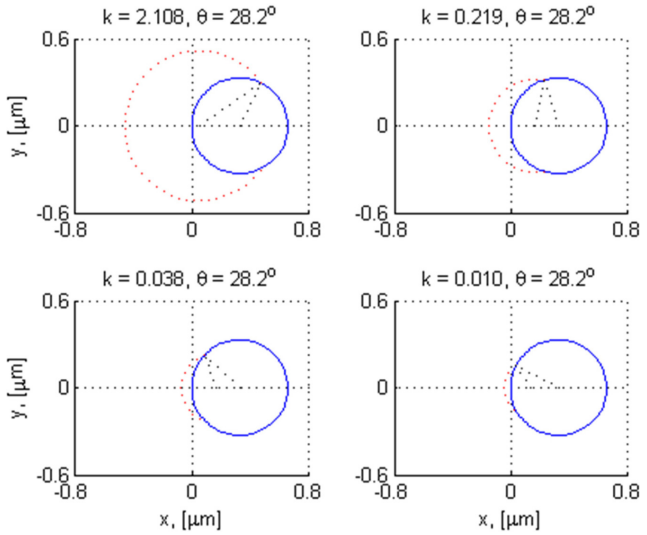

Fig. 8. The cross-sectional equilibrium configurations of the RD model with respect to the loading ratio of organics/water in nonane/water system (solid line: aqueous phase, dotted line: organic phase).

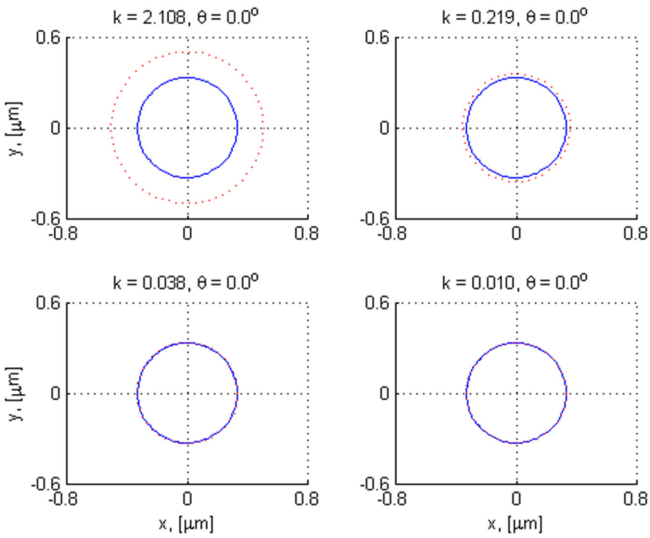

Fig. 9. The cross-sectional equilibrium configurations of the core-shell model with respect to the loading ratio of organics/water in octanol/water system (solid line: aqueous phase, dotted line: organic phase).

5. Conclusions

We studied the morphology of sub-microscale liquid-liquid separated aerosol by using the simple RD thermodynamic model. The phenomenological morphologies can be easily discriminated by using

the criteria on the surface tension and the simultaneous solution of the volume constraint Eq. (3) and Young equation, Eq. (9). And the results may explain the experimental studies about the morphologies of the complex atmospheric aerosol by the simple arguments on the surface tensions and the loading ratio of organics/water. However, we consider only the morphological variation of particle. If the morphology drives the change of chemical processes within the particle, this would not be accounted for in this work.

References

1. Maria, S. F., Russell, L. M., Gilles, M. K. and Myneni, S. C. B., "Organic Aerosol Growth Mechanisms and Their Climate-forcing Implications," *Science*, **306**, 1921-1924(2004).
2. Park, S. S., Cho, S. Y. and Kim, S. J., "Chemical Characteristics of Water Soluble Components in Fine Particulate Matter at a Gwangju Area," *Korean Chem. Eng. Res.*, **48**(1), 20-26(2010).
3. Pye, H. O. T., Murphy, B. N., Xu, L., Ng, N. L., Carlton, A. G., Guo, H., Weber, R., Vasilakos, P., Appel, K. W., Budisulistiorini, S. H., Surratt, J. D., Nenes, A., Hu, W., Jimenez, J. L., Wertz, G. I., Misztal, P. K. and Goldstein, A. H., "On the Implications of Aerosol Liquid Water and Phase Separation for Organic Aerosol Mass," *Atmos. Chem. Phys. Discuss.*, doi:10.5194/acp-2016-719 (2016).
4. Song, M., Marcolli, C., Krieger, U. K., Zuend, A. and Peter, T., "Liquid-liquid Phase Separation and Morphology of Internally Mixed Dicarboxylic Acids/Ammonium Sulfate/Water Particles," *Atmos. Chem. Phys.*, **12**, 2691-2712(2012).
5. Zawadowicz, M. A., Proud, S. R., Seppalalinen, S. S. and Cziczo, D. J., "Hygroscopic and Phase Separation Properties of Ammonium Sulfate/Organics/Water Ternary Solutions," *Atmos. Chem. Phys.*, **15**, 8975-8986(2015).
6. Shiraiwa, M., Zuend, A., Bertram, A. K. and Seinfeld, J. H., "Gas-particle Partitioning of Atmospheric Aerosols: Interplay of Physical State, Non-ideal Mixing and Morphology," *Phys. Chem. Chem. Phys.*, **15**, 11441-11453(2013).
7. Zhang, Q. and Thompson, J. E., "Effect of Particle Mixing Morphology on Aerosol Scattering and Absorption: A Discrete Dipole Modeling Study," *GeoResJ*, **3-4**, 9-18(2014).
8. De Leeuw, G., Andreas, E. L., Anguelova, M. D., Fairall, C. W., Lewis, E. R., O'Dowd, C., Schulz, M. and Schwartz, S. E., "Production of Flux of Sea Spray Aerosol," *Rev. Geophys.*, **49**(2), doi: 10.1029/2010RG000349 (2011).
9. Zuend, A., Marcolli, C., Peter, T. and Seinfeld, J. H., "Computation of Liquid-liquid Equilibria and Phase Stabilities: Implications for RH-dependent Gas/particle Partitioning of Organic-inorganic Aerosols," *Atmos. Chem. Phys.*, **10**, 7795-7820(2010).
10. Zeund, A. and Seinfeld, J. H., "Practical Method for the Calculation of Liquid-liquid Equilibria in Multicomponent Organic-water-electrolyte Systems Using Physicochemical Constraints," *Fluid Phase Equilibria*, **337**, 201-213(2013).
11. Amundson, N. R., Caboussat, A., He, J. W., Martynenko, A. V., Savarin, V. B., Seinfeld, J. H. and Yoo, K. Y., "A New Inorganic Atmospheric Aerosol Phase Equilibrium Model (UHAERO)," *Atmos. Chem. Phys.*, **6**, 975-992(2006).
12. Amundson, N. R., Caboussat, A., He, J. W., Martynenko, A. V., and Seinfeld, J. H., "A Phase Equilibrium Model for Atmospheric Aerosols Containing Inorganic Electrolytes and Organic Compounds (UHAERO), with Application to Dicarboxylic Acids," *J. Geophys. Res. Atmos.*, **112**, D24S13(2007).
13. Yu, H., Kaufman, Y. J., Chin, M., Feingold, G., Remer, L. A., Anderson, T. L., Balkanski, Y., Bellouin, N., Boucher, O., Christopher, S., DeCola, P., Kahn, R., Koch, D., Loeb, N., Reddy, M. S., Schulz, M., Takemura, T. and Zhou, M., "A Review of Measurement-based Assessments of the Aerosol Direct Radiative Effect and Forcing," *Atmos. Chem. Phys.*, **6**, 613-666(2006).
14. Qju, Y. and Molinero, V., "Morphology of Liquid-Liquid Phase Separated Aerosols," *J. Am. Chem. Soc.*, **137**, 10642-10651(2015).
15. Obeidat, A., Hrahsheh, F. and Wilemski, G., "Scattering Form Factors for Russian Doll Aerosol Droplet Models," *J. Phys. Chem. B*, **119**, 9304-9311(2015).
16. You, Y., Renbaum-Wolff, L., Carreras-Sospedra, M., Hanna, S. J., Hiranuma, N., Kamald, S., Smith, M. L., Zhang, X., Weber, R. J., Shilling, J. E., Dabdub, D., Martin, S. T. and Bertram, A. K., "Images Reveal that Atmospheric Particles can Undergo Liquid-liquid Phase Separations," *Proc. Nat'l Acad. Sci.*, **109**, 13188-13193(2012).
17. Veghte, D. P., Bittner, D. R. and Freedman, M. A., "Cryo-Transmission Electron Microscopy Imaging of the Morphology of Submicrometer Aerosol Containing Organic Acids and Ammonium Sulfate," *Anal. Chem.*, **86**, 2436-2442(2014).
18. Kwamena, N. O. A., Buajarern, J. and Reid, J. P., "Equilibrium Morphology of Mixed Organic/Inorganic/Aqueous Aerosol Droplets: Investigating the Effect of Relative Humidity and Surfactants," *J. Phys. Chem. A*, **114**, 5787-5795(2010).
19. Vargaftik, N. B., Volkov, B. N. and Voljak, L. D., "International Tables of the Surface Tension of Water," *J. Phys. Chem. Ref. Data*, **12**(3), 817-820(1983).
20. Goebel, A. and Lunkenheimer, K., "Interfacial Tension of the Water/n-Alkane Interface," *Langmuir*, **13**, 369-372(1997).